

December 13, 2005

**Systematic analysis of myotubularins: heteromeric interactions, sub-cellular localisation and endosome related functions.**

Óscar Lorenzo and Michael J. Clague\*

Physiological Laboratory, University of Liverpool, Crown St., Liverpool, L69 3BX, UK

\*corresponding author  
e-mail [clague@liv.ac.uk](mailto:clague@liv.ac.uk)

key words: myotubularin, phosphatase, yeast two-hybrid, protein-protein interactions, endosomes

running title: myotubularin interactions

word count=4575

**Abstract**

The myotubularins are a large family of lipid phosphatases with specificity towards  $\text{PtdIns}3P$  and  $\text{PtdIns}(3,5)P_2$ . Each of the 14 family members bears a signature phosphatase domain, which is inactive in six cases due to amino acid changes at the catalytic site. Fragmentary data have indicated heteromeric interactions between myotubularins, which have hitherto paired an active family member with an inactive one. In this study we have conducted a large-scale analysis of potential associations within the human myotubularin family, through directed two-hybrid screening and immunoprecipitation of epitope tagged proteins. We have confirmed all previously reported combinations and identified novel heteromeric interactions; MTMR8 with MTMR9 and MTMR3 with MTMR4, the first such combination of enzymatically active MTMs. We also report the capacity of several family members to self-associate, including MTMR3 and MTMR4. Sub-cellular localisation studies reveal a unique distribution of MTMR4 to endosomal structures, the major site of substrate lipid accumulation. All active MTMs we have tested (MTM1, MTMR2–4) reduce endosomal  $\text{PtdIns}3P$  levels upon over-expression. Amongst these, only MTMR4 induces a pronounced defect in the EGF receptor degradation pathway, which is independent of phosphatase activity, but requires an intact FYVE domain.

## Introduction

The myotubularin (MTM) family constitutes one of the largest and most highly conserved protein-tyrosine phosphatase subfamilies in eukaryotes (Alonso et al., 2004; Clague and Lorenzo, 2005). The consensus CX<sub>5</sub>R active site motif is found in the MTM family and the sequence “CSDGWDR” is invariant within all of the enzymatically active members. There are eight active members of the family, and six further members which bear inactivating mutations within the catalytic site (Laporte et al., 2003). Each myotubularin possesses an N-terminal PH-GRAM (PH-G) domain and a coiled-coil domain whilst several distinct C-terminal domains, such as PDZ or FYVE domains are represented within the family. Active members possess conserved phosphoinositide 3-phosphatase activity towards PtdIns3P and PtdIns(3,5)P<sub>2</sub> (Blondeau et al., 2000; Schaletzky et al., 2003; Taylor et al., 2000; Walker et al., 2001), which are important lipid regulators of endosomal dynamics (Roth, 2004). Mutations in MTM1 lead to myotonic myopathy (Laporte et al., 1996), whilst mutations or truncations in MTMR2 or MTMR13/Sbf2 lead to clinically indistinguishable forms of Charcot-Marie-Tooth syndrome (Azzedine et al., 2003; Berger et al., 2002; Bolino et al., 2000; Senderek et al., 2003). A recent siRNA screen has also suggested that MTMs may regulate cell survival (Mackeigan et al., 2005).

Several interactions between myotubularin family members have now been characterised through identification of co-immunoprecipitating proteins in isolated studies. Thus MTM1 and MTMR2 interact with MTMR12/3-PAP (Nandurkar et al., 2003), MTMR6 and MTMR7 with MTMR9 (Mochizuki and Majerus, 2003), whilst MTMR2 also interacts with MTMR5/Sbf1 and MTMR13/Sbf2 (Kim et al., 2003; Robinson and Dixon, 2005). Furthermore MTMR2 has been shown to dimerise through its coiled-coil domain (Berger et al., 2003; Kim et al., 2003) and MTM1 can form heptameric ring structures (Schaletzky et al., 2003). So far, all

heteromeric interactions have paired an active enzyme with an inactive enzyme, suggesting that this could constitute a “rule” which may have functional significance.

To date there has been no systematic survey of the extent of myotubularin intra-family associations. We have now tested interactions between twelve family members by directed yeast 2-hybrid screening (144 combinations) and by co-immunoprecipitation of epitope-tagged proteins expressed in HeLa cells. We confirmed all previously characterised heteromeric interactions, whilst identifying several novel interactions, most notably between two active enzymes MTMR3 and MTMR4. We also report data on the sub-cellular localisation of each protein when over-expressed and the influence that co-expression of binding partners may have on this distribution. MTMR4 shows the clearest localisation to endosomal compartments exerts a unique inhibition of EGFR degradation pathway.

## Materials and methods

### *Plasmids and strains*

Human myotubularin cDNA sequences were obtained as follows: MTM1, its catalytically inactive mutant C375S, and MTMR6 from Dr. F. Barr (Martinsreid, Germany), MTMR12 from Dr. H. Nandurkar (Monash University, Australia), MTMR2 and MTMR4 from Kazusa (Acc.Nos. AB028996 and AB014547), MTMR3 from Dr. Nagase (Chiba, Japan), MTMR5 from Dr. ML. Cleary (Stanford University, California), MTMR7 from RZPD (CR749240), MTMR8, MTMR9 and MTMR10 from the MRC mammalian gene collection (BC012399, BC022003, AL832603), MTMR11 (AK097000) from NITE (National Institute of Technology Evaluation, Japan). All of them were put into pCR4-Topo vectors (Invitrogen) and subcloned into bait (pFBT9, kanamycin resistant version of pGBT9) and prey (pACT2) vectors for directed Yeast Two Hybrid (Clontech). For expression in HeLa cells, MTM cDNAs were sub-cloned into HA- and EGFP-epitope tagging vectors (Clontech). MTMR3 mutants;  $\Delta$ PHG/C413S, C413S, truncated MTMR3 (1-821) and MTMR4 mutants C407S and C1169S were generated by Quickchange site-directed mutagenesis according to the manufacturers instructions (Stratagene), sequence verified and then sub-cloned into HA- or EGFP-epitope tagging vectors. All primer sequences are available on request.

### *Directed Yeast two-hybrid assays*

All protocols were performed as described in the yeast protocols handbook (Clontech). The yeast two-hybrid (Y2H) reporter strain *Sacharomyces Cerevisae* PJ69-4A was transformed with the various bait and prey constructs, or with the empty vectors as controls and plated on synthetic dropout media lacking tryptophan and leucine (SD-Trp/Leu). Three positive colonies of each were tested for the ability to grow on SD-

Trp/Leu/His/Ade (QDO) which would indicate an interaction between the bait and prey proteins.

### *Immunoprecipitation*

HeLa cells were transfected using Genejuice (Novagen) and lysed after 48 hours. Immunoprecipitations were performed as described previously (Urbé et al., 2003). The precipitated proteins were separated by SDS/PAGE and transferred to nitrocellulose. Immunoblotting was performed using standard techniques: the membrane was blocked with 5% (w/v) low-fat milk in PBS and washed in PBS containing 0.5% (w/v) Tween-20. Then, they were incubated overnight at 4°C with anti-HA mouse antibody (Cambridge Bioscience, MMS-10IP) and detected using secondary anti-mouse HRP coupled antibody (Sigma, A4416). Membranes were re-probed with sheep anti-EGFP (gift of Dr. Ian Prior, University of Liverpool) and anti-sheep HRP antibody (Sigma, A9452).

### *Immunofluorescence*

We used mouse anti-HA antibody (Cambridge Bioscience), rabbit anti-Hrs (Urbé et al., 2000), rabbit anti-EEA1 (Mills et al., 1998), mouse anti-Lamp2 (Hybridoma bank, Iowa) anti-EGF-R1 (CRUK) sheep anti-GM130 (Dr F.Barr, Martinsreid, Germany) and Alexa Fluor Transferrin (Roche). Secondary antibodies were from Molecular Probes (Alexa Fluor 594-coupled) and wortmannin from Sigma (W1628). The GST-2xFYVE probe was produced in bacteria and isolated with glutathione-sepharose (vector, gift of H. Stenmark, Oslo) then biotinylated with Sulfo-NHS-LC-biotin (Pierce). HeLa cells were routinely transfected using Genejuice (Novagen) and left for 48 hours with one change of medium at 24 hours. Cells were fixed with 3% paraformaldehyde (PFA, TAAB, UK) in PBS. Residual PFA was quenched with 50 mM NH<sub>4</sub>Cl/PBS. Cells were permeabilised with 0.2%

Triton X-100/PBS and blocked with 10% goat serum in PBS, except for GST-2xFYVE experiments in which cells were permeabilised with 20 $\mu$ M digitonin in 80mM PIPES pH 6.7, 5mM EGTA, 1mM MgCl<sub>2</sub> and blocked with 10% BSA. All antibody dilutions were in 5% goat serum and incubation times were 30 minutes at room temperature. Biotin-GST-2xFYVE was used at 40 $\mu$ g/ml in PIPES buffer/5% BSA. Cover slips were mounted using Mowiol and cells were viewed using a confocal microscope and analysed with the accompanying software.

## Results and discussion

Various reports have demonstrated heteromeric and homomeric interactions between myotubularin family members (Berger et al., 2003; Dang et al., 2003; Kim et al., 2003; Mochizuki and Majerus, 2003; Nandurkar et al., 2003; Robinson and Dixon, 2005; Schaletzky et al., 2003). Several lines of evidence suggest that these associations may be functionally significant: (i) increased enzyme activity through association with an inactive partner (Kim et al., 2003; Mochizuki and Majerus, 2003; Schaletzky et al., 2003) (ii) altered sub-cellular distribution through expression of binding partners (Kim et al., 2003) (iii) defects in either MTMR2 and MTMR13/Sbf2 lead to a clinically indistinguishable form of Charcot-Marie-Tooth syndrome (Robinson and Dixon, 2005). To date heteromeric interactions have been detected biochemically through co-immunoprecipitation experiments of both endogenous and over-expressed proteins. Consequently our knowledge of the specificity of interactions and promiscuity of family members is fragmentary. We have now sought to systematically survey the interactions between twelve family members through directed yeast 2-hybrid screening and follow up co-immunoprecipitation experiments.

Our results are summarised in Table 1. Notably we are able to confirm all hitherto published interactions by 2-hybrid screening. In addition we have uncovered two new combinations (Table 1, in bold); MTMR3 with 4 and MTMR8 with MTMR9. A typical plate screening for interactions with MTMR4 is shown in Figure 1. Each interaction was confirmed by co-immunoprecipitation following expression of HA- and EGFP epitope tagged proteins and compared with appropriate controls. Figure 2A shows a representative experiment of this nature, showing specific interaction between MTMR3 and MTMR4. Previous studies have ascribed a role of the coiled-coil domain in MTM interactions (Berger et al., 2003; Kim et al., 2003; Robinson and Dixon, 2005). Surprisingly then,



both the MTMR3–MTMR4 and the MTMR3 homomeric interaction is retained following deletion of the C-terminal section of MTMR3 containing both FYVE and coiled-coil domains (MTMR3 (1–821), Figure 2A). Figure 2B illustrates the specific interaction between MTMR9 and a previously identified partner MTMR6, as well as a novel interacting partner MTMR8. MTMR3 and MTMR8 both showed self-activation properties in the bait vector so could not be directly tested for binding with each other by the 2-hybrid assay. However, we did not find any interaction of these proteins by co-immunoprecipitation. In fact no interactions of MTMR8 other than with MTMR9 were found by co-immunoprecipitation. Two “novel” interactions were found in one direction only by 2-hybrid, MTMR10 with MTM1 and MTMR2. However, we were unable to confirm these unequivocally in co-immunoprecipitation experiments; at this point they must be seen as potential partnerships.

Our newly established interaction between MTMR3 and MTMR4 is the first report of a heteromeric interaction between two active family members, whilst the other interactions (MTMR8 and MTMR9, and possibly MTMR10 with MTM1 and MTMR2) expand the set of active–inactive combinations. The table of interactions also reveals that with the exception of MTMR11, each member of the MTM family included in this study has at least one heteromeric binding partner.

Previous work, from ourselves and others has shown the ability of myotubularins to self associate either into dimers (MTMR2) and/or heptameric rings (MTM1) (Berger et al., 2003; Schaletzky et al., 2003). We have confirmed these interactions by directed two-hybrid screening and in addition can add MTMR3, MTMR4, MTMR9 and MTMR12 to the collection of self-associating MTMs (Table 1 and Figure 2A). On the basis of this study homo-oligomerisation does not appear to be an absolute requirement for activity across the family, as MTMR6 has well

characterised phosphatase activity in the absence of other components (Schaletzky et al., 2003) and as indicated in Table 1 does not self-interact. Conversely, analysis of inactive point mutants (MTM1 (C375S) and MTMR3 (C413S)) indicates that phosphatase activity is not required for homo- or hetero- oligomerisation. Both mutants display the same spectrum of interactions as wild-type protein in the two-hybrid assay.

Given that MTMs share substrate specificity, how can specificity of cellular function be attained? One possible mechanism is through distinct sub-cellular localisation patterns. We have therefore undertaken the most extensive analysis to date of MTMs sub-cellular localisation. The intracellular distribution of each MTM epitope-tagged with EGFP is shown in Figure 3. Most show cytosolic staining, together with specific labelling on sub-cellular structures with varying morphologies. Similar distributions were also observed for HA-tagged proteins (not shown). MTMR6 and 8 clearly stain the nuclear envelope (Figure 3F and H), whilst uniquely there is a large pool of EGFP-MTMR2 (or HA-MTMR2, not shown) within the nucleus (Figure 3B). At lower expression levels nuclear localisation is less prominent and the distribution more closely resembles a perinuclear accumulation as described by Kim et al. (Kim et al., 2002). However nuclear staining of MTMR2 has also been clearly observed in Schwann cells (Bolino et al., 2004).

Much attention has been focused on the possible association of MTMs with endocytic compartments as this is believed to be a site of accumulation of their substrate lipids (Kim et al., 2002; Roth, 2004; Tsujita et al., 2004). Surprisingly, only MTMR4 (panel D) shows a punctate distribution that is characteristic of endosomes. We examined the co-localisation of MTMR4 with endosomal markers and find striking overlap with both EEA-1 and Hrs (Figure 4A,B), two FYVE domain-containing proteins which localise to endosomes through interactions with PtdIns3P (Gaullier et al., 1998; Urbé et al., 2000). To clearly establish that MTMR4

punctae are *bona fide* endosomes we also determined extensive co-localisation with fluorescent transferrin, which has been internalised from the external medium (Figure 4C). No co-localisation with a late endosome/lysosomal marker, LAMP-2, was observed nor with a Golgi marker (GM130) (data not shown). MTMR4 localisation to endosomes is sensitive to the PtdIns 3-kinase inhibitor wortmannin, consistent with the idea that it may associate with endosomes through interaction of its FYVE domain with PtdIns3P (Figure 4D).

We have examined the effect of over-expression of active MTMs on endosomal PtdIns3P levels, as judged by staining with a biotinylated 2xFYVE probe (Gillooly et al., 2000) applied to digitonin permeabilised cells. Expression of MTM1, MTMR2, MTMR3 or MTMR4 all resulted in substantial diminution of endosomal PtdIns3P levels as seen for control cells following treatment with wortmannin (Figure 5), whilst expression of catalytically inactive mutants such as MTMR5 or MTMR9 had no effect (not shown). Our results differ from a previous report of Kim et al. (Kim et al., 2002), who observed activity of MTM1 but not MTMR2 in similar experiments. Our results suggest that upon over-expression, MTMs can hydrolyse PtdIns3P on endosomes in the absence of specific localisation, through mass action effects. It is unclear then, why if MTMR4 hydrolyses PtdIns3P, should its localisation be wortmannin dependent?. It is possible that there may be a residual pool of endosomal PtdIns3P below the detection level of the 2xFYVE probe. In this respect it is interesting that Chaussade et al. saw loss of this probe following MTM expression without a major decrease in the cellular mass levels of PtdIns3P (Chaussade et al., 2003).

It has been reported that over-expression of MTMR2 may influence the EGFR down-regulation pathway, leading to defective receptor degradation and its accumulation in late endosomes (Tsujita et al., 2004). We have carried out a similar experiment with several active MTMs. We

see no substantial effect of MTM1, MTMR2 and MTMR3, but expression of MTMR4 leads to reduced EGFR degradation 4 hours subsequent to acute stimulation (Figure 6). Surprisingly, a catalytically inactive mutant of MTMR4 (C407S) had a similar inhibitory effect (Figure 6, G–I). However, a point mutation in the FYVE domain of MTMR4, which inhibits endosomal association (not shown) significantly reduced this inhibitory effect (Figure 6, J–L). Thus the MTMR4 FYVE domain may sequester a residual PtdIns3P pool on endosomes, which is not otherwise hydrolysed by its enzymatic activity, reducing its cellular levels low enough to suppress physiological function. Alternatively, MTMR4 may exert an altogether separate inhibitory function that requires its association with endosomes. No major effects of MTMR4 expression on Transferrin receptor cycling were detected (data not shown).

To what extent do heteromeric interactions influence sub-cellular distribution? Kim et al. previously showed that co-expression of MTMR5 leads to redistribution of MTMR2. We have previously published extensive characterisation of MTMR3 localisation, which despite possession of a FYVE domain does not associate with endosomal compartments upon over-expression (Lorenzo et al., 2005; Walker et al., 2001). Following our identification of MTMR4 as an MTMR3 binding partner and *bona fide* endosomal MTM, we asked if MTMR4 could direct MTMR3 to endosomal compartments (Figure 7). Our overriding conclusion of this co-expression experiment is that there is a redistribution of both components, neither MTMR4 or MTMR3 is completely dominant. Thus we see reduced endosomal association of MTMR4 when co-expressed with MTMR3, conversely we see some association of MTMR3 with MTMR4 associated punctae, which are presumably endosomes (Figure 5 A–C). This redistribution of HA-MTMR4 from endosomes is not seen when EGFP alone is expressed (D–F) or a non-interacting partner, MTMR10 (G–I). We have previously characterised

a mutant of MTMR3 carrying a deletion within the PH-G domain and an inactivating point mutation at the catalytic cysteine (HA-MTMR3- $\Delta$ PHG/C413S) which localises to the ribboned cisternae of the Golgi apparatus (Lorenzo et al., 2005). Co-expression of this mutant with EGFP-MTMR4 leads to the redistribution of MTMR4 to the same Golgi area, but to largely discrete structures, many of which are punctate, in close apposition to the HA-MTMR3- $\Delta$ PHG/C413S labelled Golgi (Figure 5 J-L). We propose that this represents interaction between MTMR3 and MTMR4 in trans, leading to the tethering of MTMR4 positive vesicles to the Golgi.

Does the MTMR3-dependent redistribution of MTMR4 have any functional consequence? Figure 8 shows that the previously observed inhibition of EGFR degradation due to MTMR4 over-expression is alleviated following co-expression of MTMR3, although a small number of bright punctae still remain.

In conclusion, our studies have provided at least one binding partner for eleven out of twelve MTMs. These interactions are nevertheless quite specific as no MTM shows wide-scale promiscuity. The interaction between MTMR3 and MTMR4 breaks the general trend of pairing an active with an inactive family member and may redistribute either member. Surveying the sub-cellular distribution of MTMs has led to the identification of MTMR4 as the first clear example of a MTM localising to endosomal compartments, the site of accumulation of substrate lipids.

## **Acknowledgements**

This work was supported by the Wellcome Trust. We thank Sylvie Urbé and Francis Barr for many helpful discussions.

## Table and Figure Legends

**Table 1. Protein interactions within the Myotubularin family.** MTM proteins were sub-cloned into different tagged vectors; pFBT9 (bait vector) and pACT2 (prey vector) for Directed Yeast–Two Hybrid (Y2H) screening, or into pEGFP and pCMV–HA, for co-immunoprecipitation (co-IP). Previously identified interactions are confirmed by both directed Y2H and co-IP. We also identified new interactions which are shown in bold. Grey boxes indicate active MTMs, white boxes are inactive MTMs.

**Figure 1. Directed Yeast–two hybrid interactions of MTMR4 with MTM family members.** Yeast cells were co-transfected with bait-MTMR4 and all different preys (AC). On the selective QDO plate (right), growth (interaction) was observed with MTMR3 and MTMR4 in the prey vectors (see scheme on the left). A catalytically inactive mutant of MTMR3 (C413S) retains binding to MTMR4. As a control, the same co-transformations were plated onto SD–leu/trp (centre).

**Figure 2. Co-Immunoprecipitation of human Myotubularin family members.** HeLa cells were transfected with HA-MTMR3, HA-MTMR4 or HA-MTMR9, and different EGFP-tagged myotubularins as indicated. EGFP proteins were immunoprecipitated from cell lysates and processed for Western blotting. Corresponding membranes were blotted with an anti-HA antibody (top panels) and confirmed interactions identified in the two-hybrid screen. (A) MTMR3 and MTMR4 interact with each other and with themselves. A truncated form of MTMR3–(1–821) lacking the C-terminal coiled-coil domain preserves this interaction. (B) MTMR8 interacts with MTMR9 (arrow, top panel). Membranes were re-probed with anti-EGFP (bottom panels) and lysates with an anti-HA (middle

panels) showing the efficiency of EGFP immunoprecipitation and HA-protein expression levels, respectively.

**Figure 3. Sub-cellular localization of Myotubularins in HeLa cells.**

HeLa cells were transfected for 48 hours with the different EGFP-tagged Myotubularins as indicated (A to L). Following fixation, they were examined by con-focal microscopy; representative images are shown. Scale bar represents 10  $\mu$ m

**Figure 4. MTMR4 localizes to endosomes.**

HeLa cells were transfected with EGFP-MTMR4 and co-stained after fixation with anti-EEA-1 or anti-Hrs respectively (A and B). (C) AlexaFluor-Transferrin was internalised into transfected cells during a 30 minute incubation. (D) Transfected cells were treated with wortmannin for 1hour before fixation. Scale bar represents 10  $\mu$ m.

**Figure 5. Dephosphorylation of an endosomal pool of PtdIns3P by MTMs.**

HeLa cells were transfected with MTM1 (A-C), MTMR2 (D-F), MTMR3 (G-I), MTMR4 (J-L), fixed and endosomal PtdIns3P was detected using a biotinylated-GST-2xFYVE protein. Control cells are shown in (N) and wortmannin treated cells in (M). Scale bar represents 10  $\mu$ m.

**Figure 6. MTMR4 inhibits EGFR degradation.**

HeLa cells were transfected with pHA-MTMR4 (A-C), its phosphatase inactive mutant HA-C407S (G-I), its FYVE domain mutant HA-C1169S (J-L), or pEGFP-MTMR3 (D-F). 100ng/ml EGF was added to starved cells for four hours, which were then fixed and processed for immunofluorescence of EGFR as described in materials and methods. Bars represent 10  $\mu$ m. Cells expressing MTMR4 or its phosphatase inactive mutant retain EGFR in numerous bright fluorescent punctae.

**Figure 7. MTMR4 and MTMR3 interaction leads to redistribution.** HeLa cells were co-transfected with the following combinations; (A to C) HA-MTMR4 and EGFP-MTMR3, (D to F) HA-MTMR4 and EGFP control vector, (G-I) HA-MTMR10 and EGFP-MTMR4, and (J-L) HA-MTMR3- $\Delta$ PHG/C413S and EGFP-MTMR4. Merged images are shown on the right. Scale bar represents 10  $\mu$ m.

**Figure 8. Co-expression of MTMR3 alleviates MTMR4 inhibition of EGFR degradation.** HeLa cells were co-transfected with EGFP-MTMR4 and HA-MTMR3. 100ng/ml EGF was added to starved cells for four hours, which were then fixed and processed for immunofluorescence of EGF-R1 and HA as described in materials and methods. Cells contain fewer bright EGFR containing punctae than when MTMR4 is expressed alone (see Figure 6).



## References

- Alonso, A., Sasin, J., Bottini, N., Friedberg, I., Friedberg, I., Osterman, A., Godzik, A., Hunter, T., Dixon, J. and Mustelin, T.** (2004). Protein tyrosine phosphatases in the human genome. *Cell* **117**, 699–711.
- Azzedine, H., Bolino, A., Taieb, T., Birouk, N., Di Duca, M., Bouhouche, A., Benamou, S., Mrabet, A., Hammadouche, T., Chkili, T. et al.** (2003). Mutations in MTMR13, a new pseudophosphatase homologue of MTMR2 and Sbf1, in two families with an autosomal recessive demyelinating form of Charcot–Marie–Tooth disease associated with early-onset glaucoma. *Am J Hum Genet* **72**, 1141–53.
- Berger, P., Bonneick, S., Willi, S., Wymann, M. and Suter, U.** (2002). Loss of phosphatase activity in myotubularin-related protein 2 is associated with Charcot–Marie–Tooth disease type 4B1. *Hum Mol Genet* **11**, 1569–79.
- Berger, P., Schaffitzel, C., Berger, I., Ban, N. and Suter, U.** (2003). Membrane association of myotubularin-related protein 2 is mediated by a pleckstrin homology–GRAM domain and a coiled-coil dimerization module. *Proc Natl Acad Sci U S A* **100**, 12177–82.
- Blondeau, F., Laporte, J., Bodin, S., Superti-Furga, G., Payrastre, B. and Mandel, J.–L.** (2000). Myotubularin, a phosphatase deficient in myotubular myopathy, acts on phosphatidylinositol 3–kinase and phosphatidylinositol 3–phosphate pathway. *Hum. Mol. Gen.* **9**, 2223–2229.
- Bolino, A., Bolis, A., Previtali, S. C., Dina, G., Bussini, S., Dati, G., Amadio, S., Del Carro, U., Mruk, D. D., Feltri, M. L. et al.** (2004). Disruption of Mtmr2 produces CMT4B1-like neuropathy with myelin outfolding and impaired spermatogenesis. *J Cell Biol* **167**, 711–21.
- Bolino, A., Muglia, M., Conforti, F. L., LeGuern, E., Salih, M. A., Georgiou, D. M., Christodoulou, K., Hausmanowa–Petrusewicz, I., Mandich, P., Schenone, A. et al.** (2000). Charcot–Marie–Tooth type 4B is caused by mutations in the gene encoding myotubularin-related protein-2. *Nat Genet* **25**, 17–9.
- Chaussade, C., Pirola, L., Bonnafous, S., Blondeau, F., Brenz-Verca, S., Tronchere, H., Portis, F., Rusconi, S., Payrastre, B., Laporte, J. et al.** (2003). Expression of myotubularin by an adenoviral vector demonstrates its function as a phosphatidylinositol 3–phosphate [PtdIns(3)P] phosphatase in muscle cell lines: involvement of PtdIns(3)P in insulin-stimulated glucose transport. *Mol Endocrinol* **17**, 2448–60.
- Clague, M. J. and Lorenzo, O.** (2005). The myotubularin family of lipid phosphatases. *Traffic* **6**, 1063–9.
- Dang, H., Li, Z., Skolnik, E. Y. and Fares, H.** (2003). Disease related myotubularins function in endocytic traffic in *Caenorhabditis elegans*. *Mol. Biol. Cell*.
- Gaullier, J.–M., Simonsen, A., D'Arrigo, A., Bremnes, B. and Stenmark, H.** (1998). FYVE fingers bind PtdIns(3)P. *Nature* **394**, 432–433.

**Gillooly, D. J., Morrow, I. C., Lindsay, M., Gould, R., Bryant, N. J., Gaullier, J. M., Parton, R. G. and Stenmark, H.** (2000). Localization of phosphatidylinositol 3-phosphate in yeast and mammalian cells. *EMBO. J.* **19**, 4577–4588.

**Kim, S. A., Taylor, G. S., Torgersen, K. M. and Dixon, J. E.** (2002). Myotubularin and MTMR2, phosphatidylinositol 3-phosphatases mutated in myotubular myopathy and type 4B Charcot-Marie-Tooth disease. *J Biol Chem* **277**, 4526–31.

**Kim, S. A., Vacratsis, P. O., Firestein, R., Cleary, M. L. and Dixon, J. E.** (2003). Regulation of myotubularin-related (MTMR)2 phosphatidylinositol phosphatase by MTMR5, a catalytically inactive phosphatase. *Proc Natl Acad Sci U S A* **100**, 4492–7.

**Laporte, J., Bedez, F., Bolino, A. and Mandel, J. L.** (2003). Myotubularins, a large disease-associated family of cooperating catalytically active and inactive phosphoinositides phosphatases. *Hum Mol Genet* **12 Suppl 2**, R285–92.

**Laporte, J., Hu, L. J., Kretz, C., Mandel, J.-L., Kioschis, P., Coy, J. F., Klauck, S. M., Poustka, A. and Dahl, N.** (1996). A gene mutated in X-linked myotubular myopathy defines a new putative tyrosine phosphatase family conserved in yeast. *Nature Genetics* **13**, 175–182.

**Lorenzo, O., Urbe, S. and Clague, M. J.** (2005). Analysis of phosphoinositide binding domain properties within the myotubularin-related protein MTMR3. *J Cell Sci* **118**, 2005–12.

**Mackeigan, J. P., Murphy, L. O. and Blenis, J.** (2005). Sensitized RNAi screen of human kinases and phosphatases identifies new regulators of apoptosis and chemoresistance. *Nat Cell Biol* **7**, 591–600.

**Mills, I. G., Jones, A. T. and Clague, M. J.** (1998). Involvement of the endosomal autoantigen EEA1 in homotypic fusion of early endosomes. *Current Biology* **8**, 881–884.

**Mochizuki, Y. and Majerus, P. W.** (2003). Characterization of myotubularin-related protein 7 and its binding partner, myotubularin-related protein 9. *Proc Natl Acad Sci U S A* **100**, 9768–73.

**Nandurkar, H. H., Layton, M., Laporte, J., Selan, C., Corcoran, L., Caldwell, K. K., Mochizuki, Y., Majerus, P. W. and Mitchell, C. A.** (2003). Identification of myotubularin as the lipid phosphatase catalytic subunit associated with the 3-phosphatase adapter protein, 3-PAP. *Proc Natl Acad Sci U S A* **100**, 8660–5.

**Robinson, F. L. and Dixon, J. E.** (2005). The phosphoinositide 3-phosphatase MTMR2 associates with MTMR13, a novel membrane-associated pseudophosphatase also mutated in type 4B Charcot-Marie-tooth disease. *J Biol Chem*.

**Roth, M. G.** (2004). Phosphoinositides in constitutive membrane traffic. *Physiol Rev* **84**, 699–730.

**Schaletzky, J., Dove, S. K., Short, B., Lorenzo, O., Clague, M. J. and Barr, F. A.** (2003). Phosphatidylinositol-5-phosphate activation and

conserved substrate specificity of the myotubularin phosphatidylinositol 3-phosphatases. *Curr Biol* **13**, 504–9.

**Senderek, J., Bergmann, C., Weber, S., Ketelsen, U. P., Schorle, H., Rudnik-Schoneborn, S., Buttner, R., Buchheim, E. and Zerres, K.** (2003). Mutation of the SBF2 gene, encoding a novel member of the myotubularin family, in Charcot-Marie-Tooth neuropathy type 4B2/11p15. *Hum Mol Genet* **12**, 349–356.

**Taylor, G. S., Maehama, T. and Dixon, J. E.** (2000). Myotubularin, a protein tyrosine phosphatase mutated in myotubular myopathy, dephosphorylates the lipid second messenger phosphatidylinositol 3-phosphate. *Proc. Natl. Acad. Sci.*, 9431–9436.

**Tsujita, K., Itoh, T., Ijuin, T., Yamamoto, A., Shisheva, A., Laporte, J. and Takenawa, T.** (2004). Myotubularin regulates the function of the late endosome through the gram domain-phosphatidylinositol 3,5-bisphosphate interaction. *J Biol Chem* **279**, 13817–24.

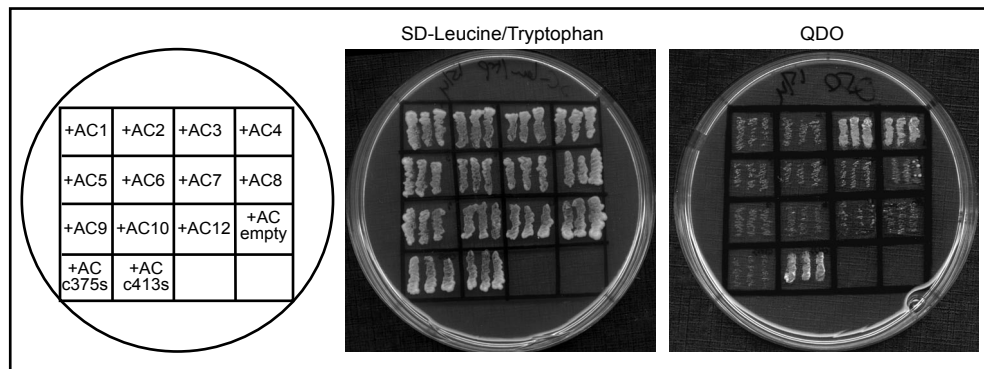
**Urbé, S., Mills, I. G., Stenmark, H., Kitamura, N. and Clague, M. J.** (2000). Endosomal localization and receptor dynamics determine tyrosine phosphorylation of hepatocyte growth factor-regulated tyrosine kinase substrate. *Mol Cell Biol* **20**, 7685–92.

**Urbé, S., Sachse, M., Row, P. E., Preisinger, C., Barr, F. A., Strous, G., Klumperman, J. and Clague, M. J.** (2003). The UIM domain of Hrs couples receptor sorting to vesicle formation. *J. Cell Sci.* **116**, 4169–4179.

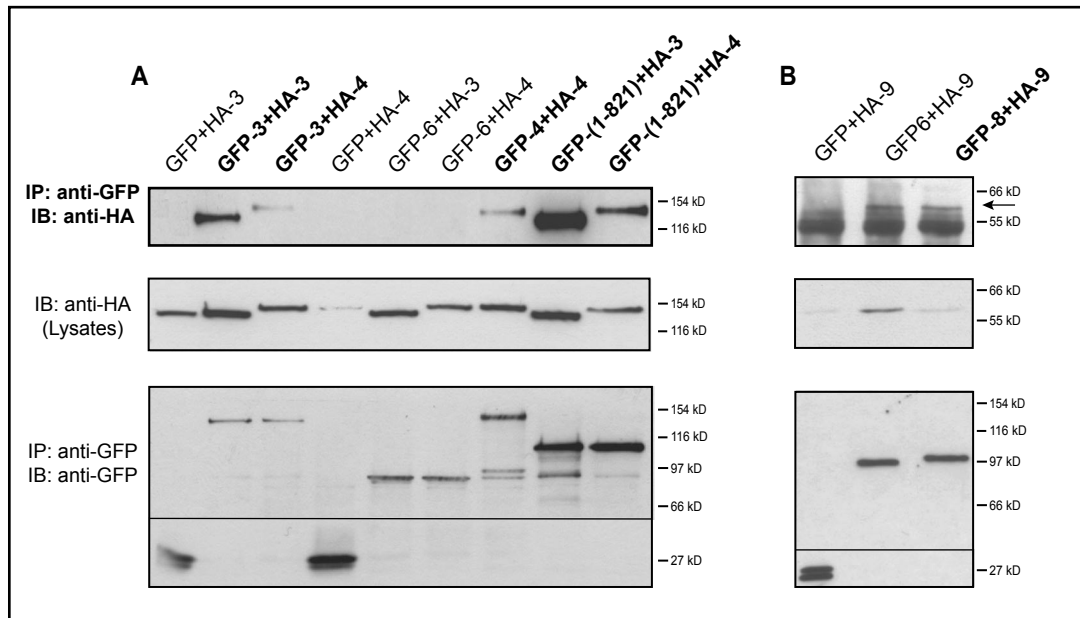
**Walker, D. M., Urbe, S., Dove, S. K., Tenza, D., Raposo, G. and Clague, M. J.** (2001). Characterization of MTMR3. an inositol lipid 3-phosphatase with novel substrate specificity. *Curr Biol* **11**, 1600–5.

	Directed Y2H Bait-Prey	Directed Y2H Prey-Bait	co-IP	<i>Previous data (by co-IP)</i>
hMTM1	1, 12	1, 12	1, 12	1, 12
hMTMR1	not done	not done	not done	
hMTMR2	2, 5, 12	2, 5, 12	2, 5, 12	2, 5, 12, 13
hMTMR3	(self activated)	<b>4</b>	<b>3, 4</b>	
hMTMR4	<b>3, 4</b>	<b>3, 4</b>	<b>3, 4</b>	
hMTMR5	2	2	2	2
hMTMR6	9	9	9	9
hMTMR7	9	9	9	9
hMTMR8	(self activated)	<b>9</b>	<b>9</b>	
hMTMR9	6, 7, <b>8, 9</b>	6, 7, <b>9</b>	6, 7, <b>8</b>	6, 7
hMTMR10	<b>1, 2</b>	-	<b>1, 2</b>	
hMTMR11	-	-		
hMTMR12	1, 2, <b>12</b>	1, 2, <b>12</b>	1, 2	1, 2
hMTMR13	not done	not done	not done	2

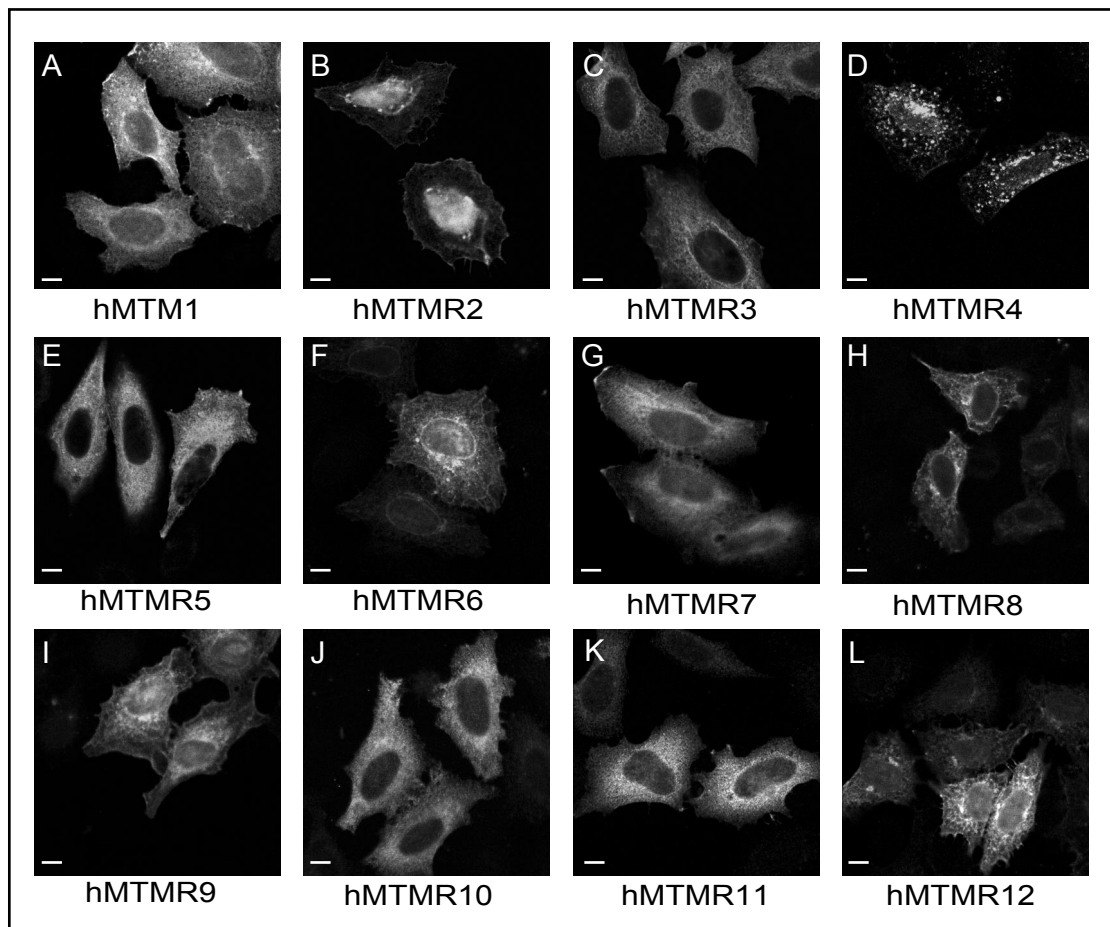
*Lorenzo et al.* **Table 1**



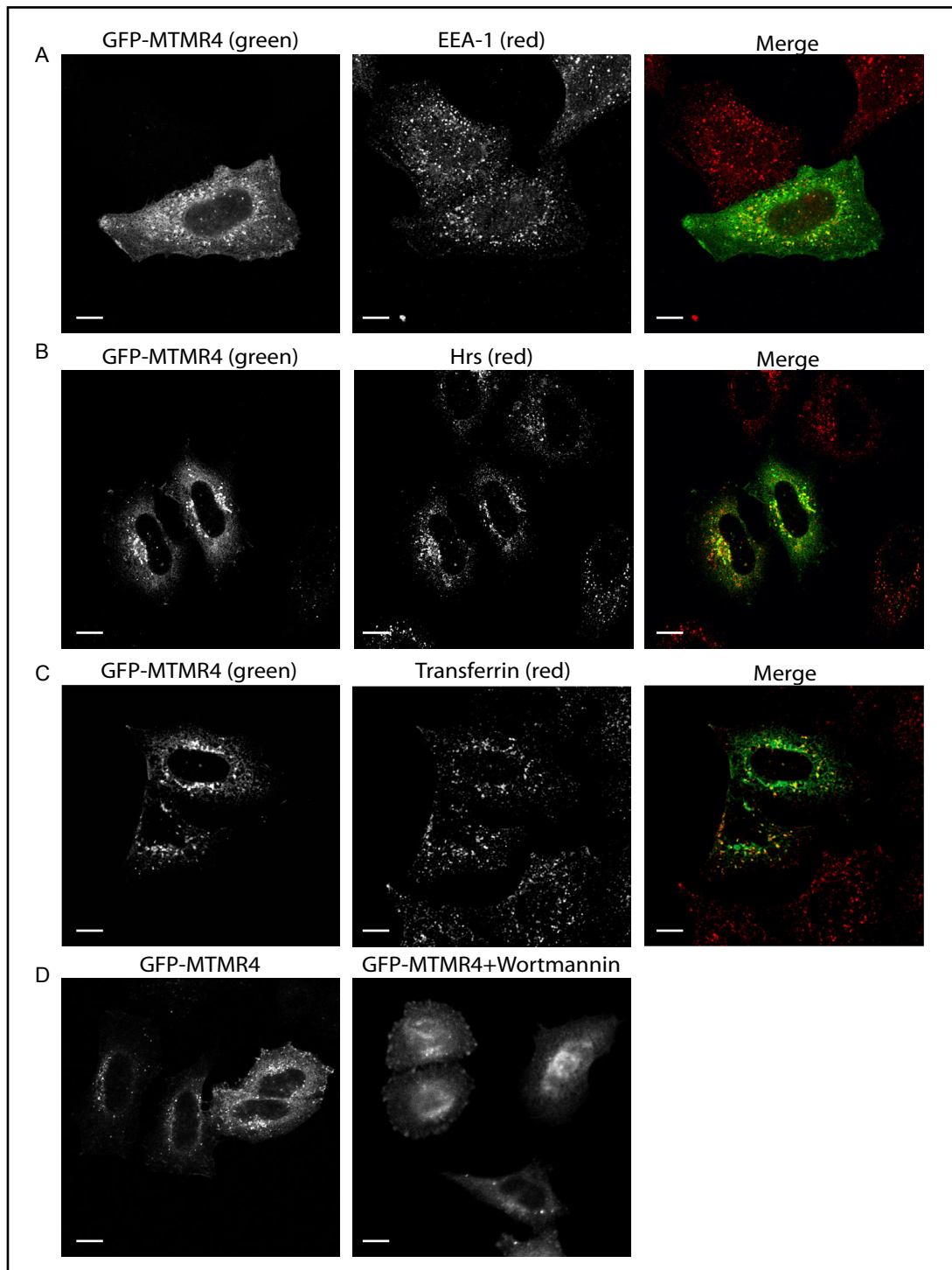
*Lorenzo et al. Figure 1*



*Lorenzo et al. Figure 2*

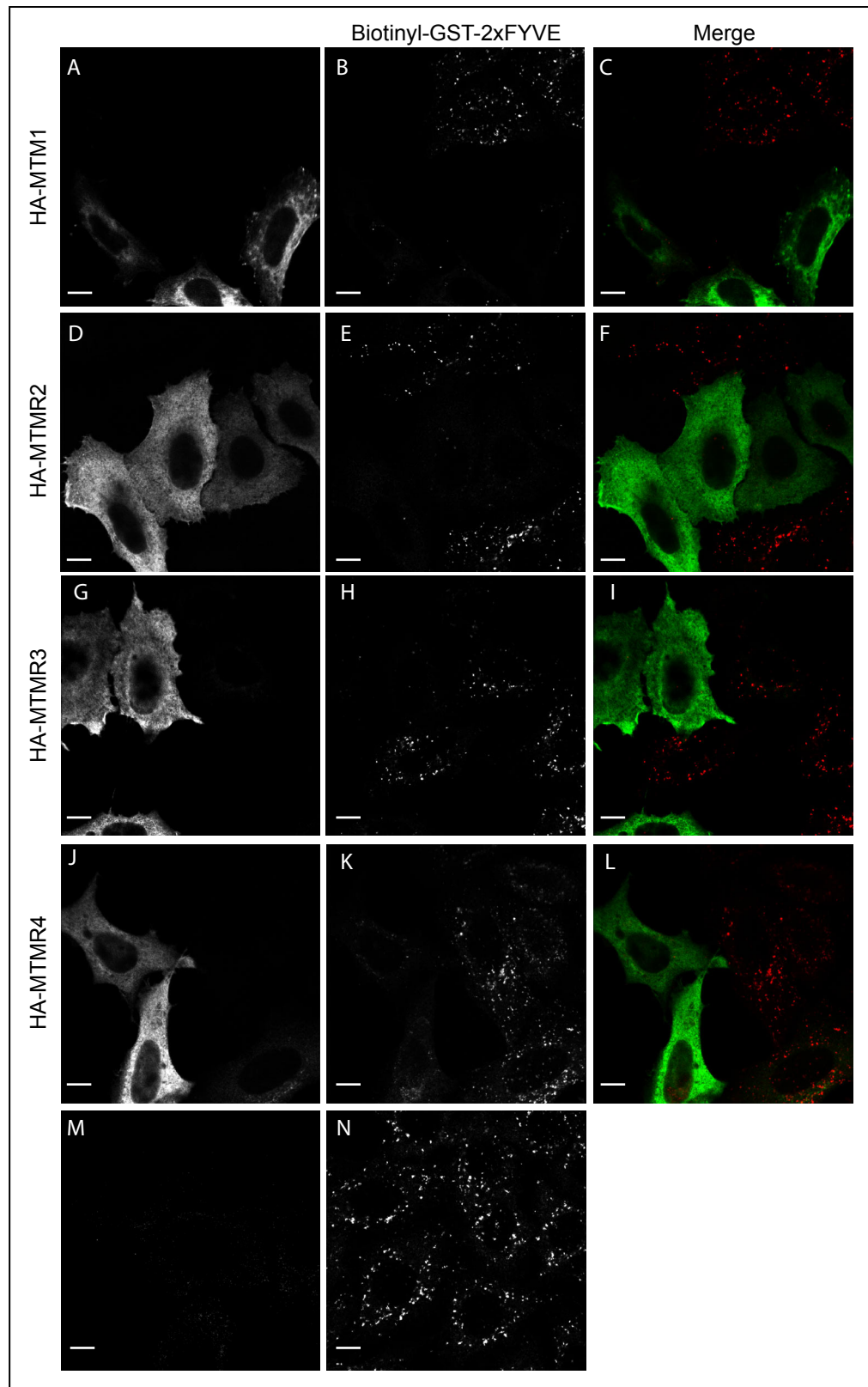


*Lorenzo et al. Figure 3*

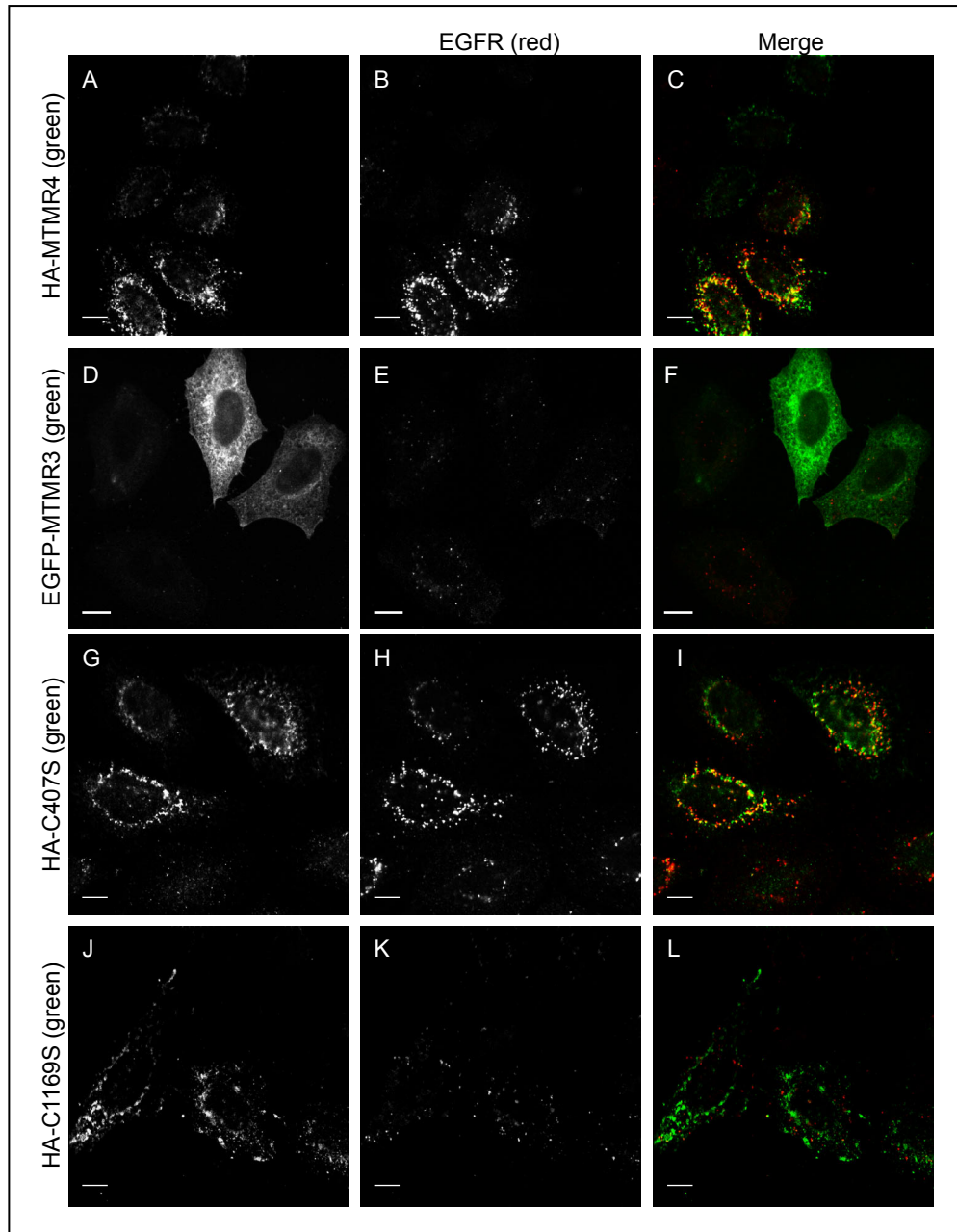


*Lorenzo et al. Figure 4*

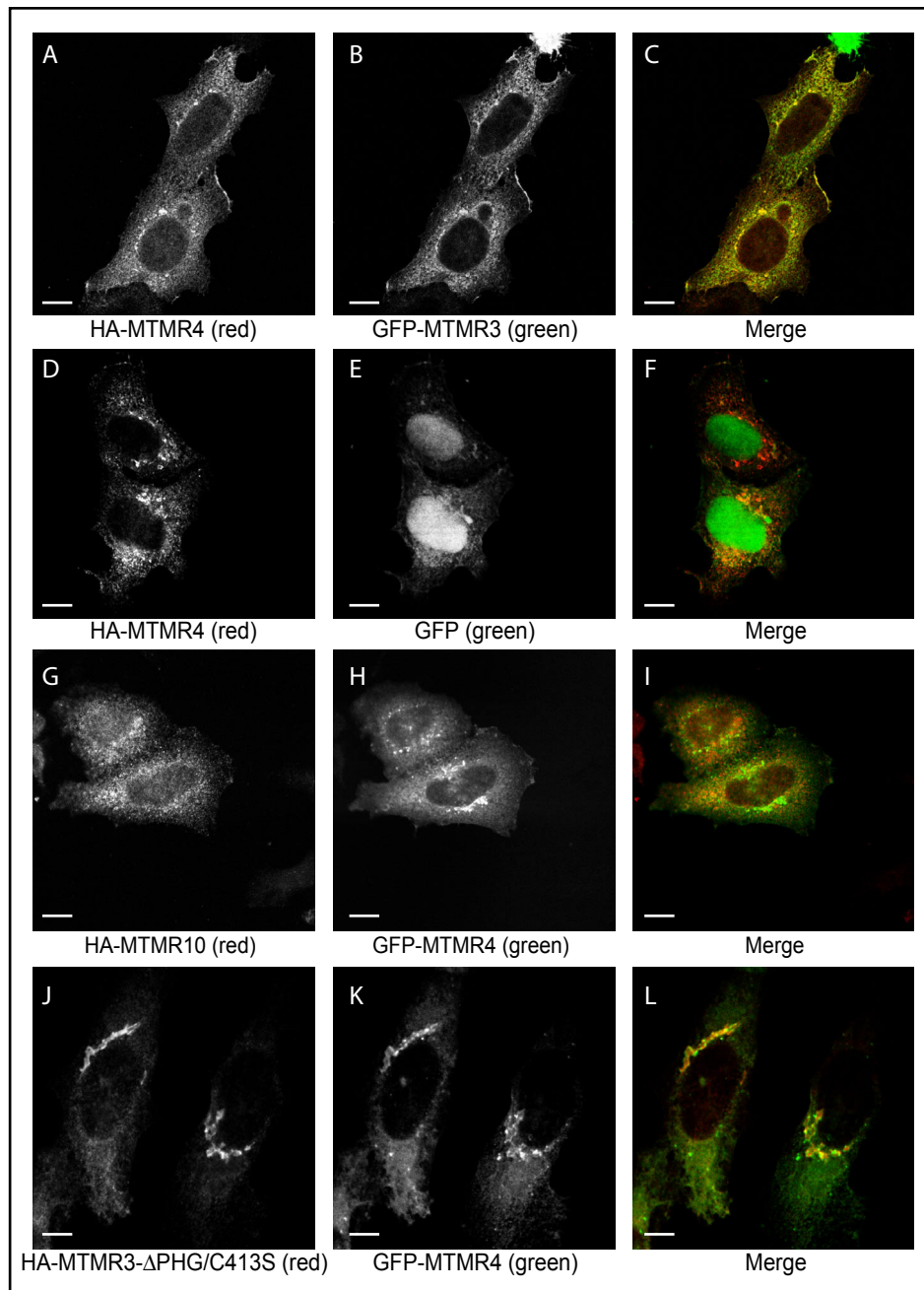




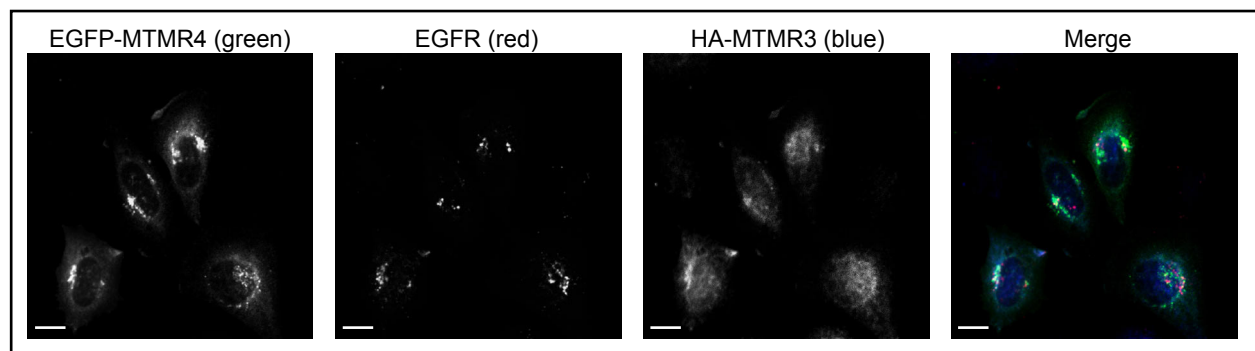
*Lorenzo et al. Figure 5*



*Lorenzo et al.* Figure 6



*Lorenzo et al. Figure 7*



*Lorenzo et al.* **Figure 8**